Influence of Pendant Chains on Mechanical Properties of Model Poly(dimethylsiloxane) Networks. 2. Viscoelastic Properties

Marcelo A. Villar and Enrique M. Vallés*

Planta Piloto de Ingeniería Química, UNS−CONICET, 12 de Octubre 1842, 8000 Bahía Blanca, Argentina

Received May 16, 1995; Revised Manuscript Received January 16, 1996[⊗]

ABSTRACT: Viscoelastic properties of model poly(dimethylsiloxane) networks with pendant chains composed of linear molecules of known and uniform molecular weights are studied. It was found that the loss modulus (G'') of these networks depends on the concentration and the molecular weight of the dangling chains. The dependency of the relaxation times of pendant chains on their molecular weights, proposed by de Gennes, was verified using the values of G'' measured experimentally. Elastic properties of these networks decrease due to the presence of the pendant chains. This results in a reduction in the amount of elastically active chains. Low-frequency elastic moduli of the networks are coincident with equilibrium values predicted by the theory of rubber elasticity, provided that the contribution of trapped entanglements is taken into account. Values of elastic moduli obtained from swelling experiments also show excellent agreement with theoretical values.

I. Introduction

Model silicone networks have been extensively utilized to explain the influence of molecular structure on mechanical properties. Most of the work with these networks has been focused on testing the theory of rubber elasticity and the contribution of entanglements to the elastic modulus.[1−8] The rubber elasticity theory considers that networks are formed from Gaussian chains joined at their ends by cross-linking points. Network chains can assume all possible configurations, allowed by the free rotation of the covalent unions of the chain segments, independently of the surrounding chains. This assumption implies that the molecules do not interact with their neighbors. In a real situation, several possible configurations for one chain will be inaccessible due to the presence of neighboring chains. The original version of the rubber elasticity theory is usually called "phantom" theory,[9] due to the immaterial characteristic assigned to the network chains. For this theory, the shear equilibrium modulus (G) for networks prepared in bulk can be expressed as

$$G = (\nu - \mu)RT \tag{1}$$

where R is the gas constant, T the absolute temperature, and ν and μ the concentrations of elastically active chains and of cross-linking points, respectively.

Cross-linking points in a phantom network can fluctuate around their mean positions due to Brownian motion. The higher the junction functionality, the lower will be the fluctuations. A manifestation of topological interactions among one chain and its neighbors can be the suppression of these fluctuations. If all junction fluctuations are suppressed, the following expression is obtained for small strain shear modulus:[9]

$$G = \nu RT \tag{2}$$

The same result is obtained assuming that the microscopic deformation of the junction points is affined to the macroscopic deformation of the rubber.[10] To allow for a partial fluctuation of the junction points, Dossin and Graessley[11] proposed the following expression, which gives an intermediate behavior:

$$G = (\nu - h\mu)RT \tag{3}$$

Here, h is an empirical parameter that can vary between 0 and 1. Adopting limiting values, eq 3 can be reduced to eqs 2 and 1, respectively.

Another approach is to consider that topological interactions behave as additional cross-links, contributing in an additive way to the elastic modulus values provided by the phantom network theory. This idea comes from the observation that linear polymers of relatively high molecular weight present a constant elastic modulus over a wide time scale when they are subjected to viscoelastic tests.[12,13] Explanation for this plateau in the viscoelastic behavior was based on the formation of a temporary network originating from molecular entanglements that do not relax on the time scale used in experimental measurements. Entanglements will be permanently trapped during the process of network formation. Langley[14] and Graessley and coworkers[11,15] have suggested that the contribution of trapped entanglements can be added to the equilibrium modulus, leading to another equation for the shear modulus:

$$G = (\nu - h\mu)RT + G_e T_e \tag{4}$$

where T_e is the fraction of trapped entanglements in the network and G_e is the maximum contribution to the modulus due to trapped entanglements. It is expected that G_e should be close to $G_N°$ (plateau modulus from experiments on linear chains). Theoretical calculations as well as experimental measurements indicate that $G_e \approx 0.8G_N°$.[1,16]

Many researchers have tried to elucidate the influence of elastically active chains and trapped entanglements on equilibrium properties. In contrast, very little work has focused on the influence of network defects on nonequilibrium properties. In particular, pendant chains have a strong influence on viscoelastic properties.

The basic idea, proposed by de Gennes,[17] is that linear chains are free to reptate. On the other hand, branched chains or pendant chains must relax by a different, slower mechanism, with movements from the free end to the fixed one. In pendant chains, the relaxation time increases exponentially with the number of entanglements, while it varies in a power fashion for linear molecules. Branched or pendant chains must contrib-

[⊗] Abstract published in *Advance ACS Abstracts,* April 1, 1996.

S0024-9297(95)00660-7 CCC: $12.00

ute, then, to viscoelastic properties for frequencies greater than the inverse of reptation times.[18] Particularly, Tsenoglou[16] and Curro and Pincus[18] developed models for the relaxation of pendant chains in random cross-linked networks.

To explain from a molecular point of view how concentrations and molecular weights of pendant chains affect viscoelastic properties, Bibbó and Vallés followed the evolution of the loss modulus (G'') with the extent of reaction during the curing of a difunctional, vinyl-terminated poly(dimethylsiloxane) (α,ω-PDMS) and a trifunctional cross-linker.[2] It was observed that G'' increases steadily after the gel point until a maximum value is reached, and then G'' decreases up to a final definite value when the maximum extent of reaction is attained. Maximum values of G'' were coincident with the extent of reaction at which the maximum amount of pendant chains was present in the network. The principal disadvantage of this kind of experiment lies in the impossibility of changing concentration, molecular weight, and degree of branching of the pendant chains independently because the material is generated in a random cross-linking process.

In this work, we present viscoelastic properties of model networks with controlled amounts of linear pendant chains of known molecular weight, based on a new system. This information is obtained by adding known amounts of monodisperse linear molecules of different molecular weights bearing only one vinyl end group, ω-PDMS (B_1), to the former system of α,ω-PDMS (B_2) and a trifunctional (A_3) or tetrafunctional (A_4) cross-linker.[19] At complete reaction, the concentrations of pendant chains in the network will depend on the initial composition of reactants. Provided that an appropriate selection of the reaction conditions is made in accordance with the ideas discussed in our previous paper,[21] pendant chains in the network will be composed mainly of the linear monodisperse ω-PDMS used in the reaction.

II. Experimental Section

Model silicone networks were obtained by the hydrosilation reaction, based on the addition of hydrogen silanes from the cross-linker molecules to end vinyl groups present in the prepolymer molecules.[1] One commercial difunctional prepolymer (D1) (Dow Corning) and five monodisperse monofunctional prepolymers (M1−M5) with different molecular weights were used. A Pt salt was employed to catalyze the cross-linking reaction. Monofunctional molecules were synthesized by anionic polymerization using *n*-butyllithium as initiator and *n*-hexane as solvent, which allowed us to obtain a narrow molecular weight distribution of polymers.[20] Two cross-linkers were used: phenyltris(dimethylsiloxy)silane (A_3), and tetrakis-(dimethylsiloxy)silane (A_4) (Petrarch Systems Inc.). The results of the molecular characterization of the prepolymers, as well as a description of the other reactants used in the cross-linking reactions, are given in Table 1.

Prepolymers as well as cross-linker agents were weighed in order to obtain stoichiometrically balanced mixtures with different amounts of monofunctional chains. Reactants were mixed with a mechanical stirrer and degassed under vacuum to eliminate bubbles. The reactive mixture was then placed between the plates of a Rheometrics mechanical spectrometer. The cure reaction was carried out between the plates at 40 °C. After 24 h, final properties were measured. A frequency sweep between 0.01 and 100 rad/s was done at different temperatures between −30 and 150 °C. Nitrogen was used in the environmental chamber for measurements at −30, −20, 0, and 10 °C, and air was used for temperatures of 20, 40, 60, 80, 100, 120, 140, and 150 °C. All measurements were carried out in simple shear dynamic experiments with deformations of up to 25%, within the range of linear viscoelastic response. Table 2 shows the nomenclature and compositions of prepared networks. The first letter and number identify the type of pendant chain incorporated into the system, the second letter and number stand for the functionality of the cross-linker used in the networks, and the third number is the concentration by weight of pendant chains added to the reacting mixture.

After viscoelastic measurements, networks were subjected to extraction of solubles using toluene as solvent. Samples were weighed and placed in glass jars with solvent to remove the non-cross-linked polymer. The extraction of solubles was carried out at room temperature for about 1 month, and solvent was replaced every 3 or 4 days. Following extraction, samples were weighed, and the degree of swelling was obtained. Samples were then dried under vacuum at 40 °C until complete solvent removal was achieved. Dry networks were weighed again, and weight fraction of solubles (W_s) and equilibrium degree of swelling (v_{2m}) were calculated; these are given in Table 3.

Table 1. Reactants Used in the Synthesis of PDMS Networks with Pendant Chains

polymer[a]	M_n (FTIR)	M_n (GPC)	M_w (LALLS)	M_w (GPC)	M_w/M_n (GPC)
D1		10 800		23 900	2.21
M1	21 200	24 200	26 900	26 500	1.08
M2	46 300	47 800	52 400	51 300	1.07
M3	47 000	53 100	63 600	60 600	1.14
M4	61 500	67 600	101 100	83 500	1.20
M5	96 600	97 800	128 700	121 300	1.24
cross-linkers					
A_3			$(HSi(CH_3)_2O)_3SiC_6H_5$		
A_4			$(HSi(CH_3)_2O)_4Si$		
catalyst			*cis*-$Pt((C_2H_5)_2S)_2Cl_2)$		

[a] D1, difunctional prepolymer α,ω-PDMS (B2) (includes 3.1% nonreactive polymer). M*i*, monofunctional prepolymers ω-PDMS (B1).

Table 2. Formulations Analyzed

sample	cross-linker	r = [A]/[B]	W_{B_1}
00−F3−0	A_3	1.002	
00−F3−0	A_3	1.000	
00−F4−0	A_4	1.003	
M1−F3−20	A_3	1.013	0.202
M2−F3−20	A_3	1.010	0.201
M3−F3−20	A_3	1.053	0.199
M4−F3−20	A_3	1.038	0.201
M5−F3−20	A_3	1.026	0.199
M1−F4−20	A_4	1.030	0.217
M2−F4−20	A_4	1.015	0.203
M3−F4−20	A_4	1.025	0.209
M4−F4−20	A_4	1.036	0.214
M5−F4−20	A_4	1.005	0.221
M1−F3−33	A_3	1.038	0.331
M2−F3−33	A_3	1.020	0.323
M3−F3−33	A_3	1.032	0.319
M4−F3−33	A_3	1.038	0.349
M5−F3−33	A_3	1.041	0.344
M1−F4−33	A_4	1.013	0.281
M2−F4−33	A_4	1.011	0.337
M3−F4−33	A_4	1.066	0.338
M4−F4−33	A_4	0.973	0.331
M5−F4−33	A_4	0.979	0.334

III. Results and Discussion

III.1. Network Molecular Structure. Details of final network structure were calculated using the recursive method described in the preceding paper.[21] Molecular parameters such as the weight fractions or the molecular weights of pendant chains were obtained as a function of the initial weight fraction of monofunctional chains (W_{B_1}) added to the reacting mixture. Calculations were made for stoichiometrically balanced networks with trifunctional and tetrafunctional cross-

Table 3. Weight Fraction of Solubles, Maximum Extent of Reaction Calculated, and Volume Fraction of Polymer in Networks Swollen with Toluene

sample	cross-linker	W_s	p_{fin}	v_{2m}
00−F3−0	A_3	0.006	0.940	0.224
00−F3−0	A_3	0.008	0.942	0.227
00−F4−0	A_4	0.004	0.937	0.251
M1−F3−20	A_3	0.049	0.905	0.178
M2−F3−20	A_3	0.043	0.904	0.184
M3−F3−20	A_3	0.041	0.883	0.193
M4−F3−20	A_3	0.038	0.893	0.191
M5−F3−20	A_3	0.039	0.897	0.189
M1−F4−20	A_4	0.042	0.863	0.208
M2−F4−20	A_4	0.051	0.850	0.197
M3−F4−20	A_4	0.038	0.868	0.216
M4−F4−20	A_4	0.030	0.877	0.218
M5−F4−20	A_4	0.036	0.884	0.212
M1−F3−33	A_3	0.092	0.890	0.143
M2−F3−33	A_3	0.070	0.895	0.151
M3−F3−33	A_3	0.078	0.882	0.164
M4−F3−33	A_3	0.076	0.877	0.164
M5−F3−33	A_3	0.075	0.876	0.166
M1−F4−33	A_4	0.056	0.867	0.189
M2−F4−33	A_4	0.069	0.855	0.179
M3−F4−33	A_4	0.062	0.832	0.190
M4−F4−33	A_4	0.054	0.900	0.185
M5−F4−33	A_4	0.059	0.853	0.173

linkers (A_3 and A_4), using the molecular weight of the difunctional polymer D1 and the different M*i* monofunctional chains. As a general rule, they show that, for stoichiometrically balanced mixtures with low content of monofunctional chains, it is possible to obtain a completely reacted network with linear pendant chains whose molecular weight is similar to the original molecular weight of the monofunctional (B_1) chains. Formulations with a higher amount of monofunctional chains lead to branched pendant chains, which complicate the analysis of viscoelastic properties. Results also demonstrate that the higher the molecular weight of monofunctional chains added to the mixture, the higher the amount (on a weight basis) that may be incorporated into the network maintaining a linear structure in the pendant chains.

Information about the structure of pendant chains can be obtained by looking at the evolution of the weight-average molecular weight of the pendant chains (M_{wp}) as a function of the weight fraction of monofunctional chains added to the reactive mixture (W_{B_1}). Figure 1 shows that M_{wp} remains almost constant in a considerable range of W_{B_1} values when B_1 chains have a relatively high molecular weight. In such a case, the weight-average molecular weight of the pendant chains is also coincident with the value of the weight-average molecular weight of the added monofunctional chains. This indicates that, under the prevailing reaction conditions, pendant chains are mostly linear, with negligible amounts of branched structures.

If the concentration of monofunctional chains in the reactive mixture increases, the weight-average molecular weight of pendant chains also increases. Since the only way that pendant chains can grow in size and weight is by incorporating bifunctional B_2 type chains into their structure, the calculations shown in Figure 1 indicate that, with high concentrations of monofunctional chains, networks contain a mixture of branched and linear pendant chains. Those branched pendant chains produce an increase in M_{wp} relative to the molecular weight of monofunctional chains. The presence of branched pendant chains appears at lower values of W_{B_1} if monofunctional chains have a molecular

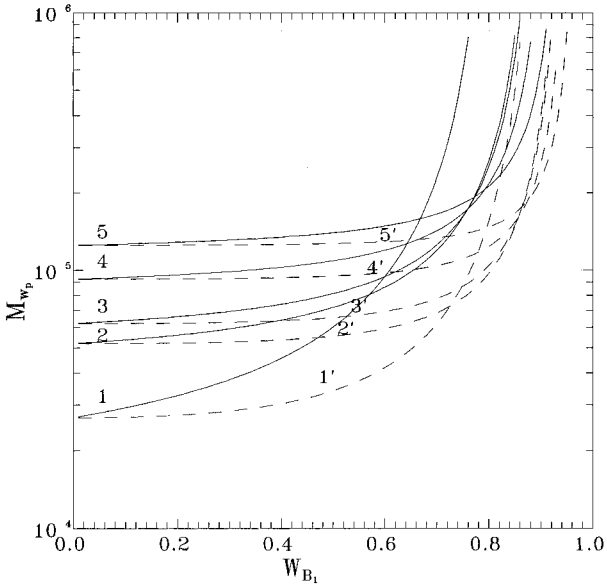

Figure 1. Weight-average molecular weight of pendant chains (M_{wp}) as a function of weight fraction of monofunctional chains (W_{B_1}). Solid lines represent networks prepared with a trifunctional cross-linker, and dashed lines those synthesized with a tetrafunctional one. Curves 1 and 1′ correspond to networks with monofunctional chains M1, 2 and 2′ to M2, 3 and 3′ to M3, 4 and 4′ to M4, and 5 and 5′ to M5. Difunctional chains used in the calculations were D1 type.

weight similar to those of the corresponding difunctional molecules in the network.

III.2. Equilibrium Swelling. Equilibrium swelling of the networks was interpreted using the Flory−Rehner equation:[10,22,23]

$$\nu - \mu = \frac{\ln(1 - v_{2m}) + v_{2m} + v_{2m}^{2}\chi_1}{V_1\left(\frac{2}{f}v_{2m} - v_{2m}^{1/3}\right)} \qquad (5)$$

where V_1 is the molar volume of the solvent, f the functionality of the cross-linking point, and χ_1 the polymer−solvent interaction parameter.

Table 4 compares values of $\nu - \mu$ obtained from eq 5 using toluene at 25 °C, and the corresponding theoretical values (with and without entanglements), calculated by a recursive technique, based on formulation data and taking into account the weight fraction of solubles measured experimentally to calculate the final extent of reaction (p_{fin}). For all calculations, a $G_e = G_N°$ value was used, assuming 0.211 MPa as the plateau modulus of PDMS.[1] Values of $\nu - \mu$ given by eq 5 are very sensitive to χ_1. In the calculations, we have used experimental values reported by Gottlieb and Herskowitz.[24]

A comparison between experimental and theoretical values indicates that, in order to explain experimental results, it is necessary to incorporate the contribution of entanglements to equilibrium elastic properties. Values of $\nu - \mu$ calculated considering trapped entanglements present a very good agreement with experimental values. On the other hand, theories that do not consider the influence of trapped entanglements clearly underpredict the experimental values. In a recent publication, Patel et al.[25] found that networks synthesized using a difunctioinal prepolymer and a tetrafunctional cross-linker exhibit similar behavior. However, a departure from the predicted theoretical values was observed when monofunctional chains were added.

Table 4. Equilibrium Degree of Swelling and Number of Elastically Active Chains Predicted by Flory−Rehner Theory and Calculated from Initial Formulation Data, Taking into Account the Weight Fraction of Solubles Obtained in Extraction Experiments

			$\nu - \mu$ (mol/m^3)		
sample	v_{2m}	$\chi_1{}^{24}$	exptl (eq 5)	calcd without entanglements[a]	calcd with entanglements[b]
00−F3−0	0.224	0.51	82.44	19.49	78.59
00−F3−0	0.227	0.51	86.07	18.41	74.35
00−F4−0	0.251	0.52	97.85	34.02	97.33
M1−F3−20	0.178	0.49	52.77	9.76	46.93
M2−F3−20	0.184	0.49	58.03	10.73	50.80
M3−F3−20	0.193	0.50	58.79	10.58	51.88
M4−F3−20	0.191	0.50	56.96	11.13	53.97
M5−F3−20	0.189	0.50	55.18	11.26	53.44
M1−F4−20	0.208	0.50	68.60	17.44	59.08
M2−F4−20	0.197	0.50	58.31	16.64	52.76
M3−F4−20	0.216	0.51	67.91	19.01	62.62
M4−F4−20	0.218	0.51	69.93	20.81	70.17
M5−F4−20	0.212	0.51	64.01	19.90	64.87
M1−F3−33	0.143	0.48	33.04	6.27	32.92
M2−F3−33	0.151	0.48	38.16	7.95	41.57
M3−F3−33	0.164	0.48	47.61	7.40	37.85
M4−F3−33	0.164	0.48	47.61	7.44	40.04
M5−F3−33	0.166	0.49	43.29	7.65	40.22
M1−F4−33	0.189	0.50	51.55	14.97	52.64
M2−F4−33	0.179	0.49	50.25	13.59	48.77
M3−F4−33	0.190	0.50	52.36	13.82	51.53
M4−F4−33	0.185	0.49	55.13	16.39	57.25
M5−F4−33	0.173	0.49	45.68	12.55	41.55

[a] $\nu - \mu$. [b] $\nu - \mu + T_e G_e/RT$. Values of ν and μ were calculated from initial formulation using the recursive method.[1]

III.3. Nonequilibrium Viscoelasic Properties. Master curves of elastic modulus (G') and loss modulus (G'') were obtained by time−temperature superposition on G' and G'' data measured at different temperatures. Superposition was carried out using the cure reaction temperature as the reference temperature (40 °C). Master curves allow the increase of the frequency ranges from 10^{-3} to 10^3 rad/s at the reference temperature. Those master curves were obtained using IRIS (innovative rheological interface software), which can also be used to calculate material properties as well as relaxation and retardation spectra corresponding to a specific polymeric material.[26] Two factors are obtained from the time−temperature superposition: the frequencies shift factor (a_T), which gives fundamentally the temperature dependence of the friction coefficient of chain segments, and the modulus shift factor (b_T), which takes into account changes in density and temperature.

Two relationships are often used to explain the dependence of a_T on temperature.[12] An Arrhenius-type dependency, in which an activation energy is obtained as a characteristic parameter, can be expressed as follows:

$$a_T = \exp\left[\frac{E_a^*}{R}\left(\frac{1}{T} - \frac{1}{T_0}\right)\right] \quad (6)$$

where E_a^* is the flow activation energy, T the absolute temperature, T_0 the reference temperature, and R the gas constant. Another way to express the functionality of a_T with temperature is to use the Williams, Landel, and Ferry (WLF) equation, which is based on the free volume changes that the material undergoes when temperature is changed.[27] In this case, a_T adopts the following expression:

$$\log a_T = \frac{-C_1^\circ (T - T_0)}{C_2^\circ + T - T_0} \quad (7)$$

Table 5. Experimental and Calculated Values of a_T and b_T

	a_T			b_T	
T (K)	exptl	Arrhenius[a]	WLF[b]	exptl	T_0/T
243	2.51×10^1	2.55×10^1	2.25×10^1	1.29	1.29
253	1.41×10^1	1.44×10^1	1.32×10^1	1.23	1.24
273	5.01	5.20	4.99	1.14	1.15
283	3.16	3.29	3.21	1.10	1.11
293	2.00	2.15	2.13	1.07	1.07
313	1.00	1.01	1.01	1.0	1.0
333	5.01×10^{-1}	5.09×10^{-1}	5.10×10^{-1}	0.93	0.94
353	2.82×10^{-1}	2.80×10^{-1}	2.79×10^{-1}	0.87	0.89
373	1.59×10^{-1}	1.64×10^{-1}	1.62×10^{-1}	0.81	0.84
393	1.00×10^{-1}	1.01×10^{-1}	9.87×10^{-2}	0.77	0.80
413	6.31×10^{-2}	6.57×10^{-2}	6.29×10^{-2}	0.73	0.76
423	5.01×10^{-2}	5.37×10^{-2}	5.10×10^{-2}	0.71	0.74

[a] E_a^*/R[K] = 3520 ± 35. [b] $C_1^\circ = 5.40 \pm 0.11$ and C_2° [K] = 349.5 ± 7.

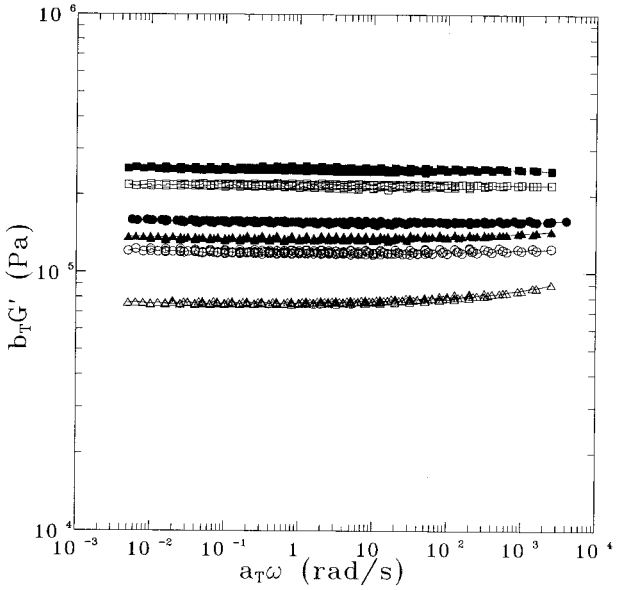

Figure 2. Master curves of elastic modulus (G') as a function of frequency (ω). $T_0 = 313$ K. Networks with monofunctional chains M1: (■) without pendant chains, tetrafunctional cross-linker; (□) without pendant chains, trifunctional cross-linker; (●) with 20 wt % of monofunctional chains, tetrafunctional cross-linker; (○) with 20 wt % of monofunctional chains, trifunctional cross-linker; (▲) with 33 wt % of monofunctional chains, tetrafunctional cross-linker; and (△) with 33 wt % of monofunctional chains, trifunctional cross-linker.

where C_1° and C_2° are temperature-independent constants. Table 5 shows a set of representative experimental values and those obtained through an Arrhenius or WLF relationship for PDMS networks measured between −30 and 150 °C (using 40 °C as reference temperature). Both models represent the dependence of a_T on temperature very satisfactorily. A comparison of a_T values obtained for PDMS networks and melts indicates that networks are more temperature dependent than melts.[12] PDMS networks studied present an elastic modulus that is almost frequency independent. For this reason, in order to get a good superposition, it is necessary to take into acocunt the changes in density and temperature of the sample. Modulus shift factors (b_T) follow the classical dependence with temperature ($b_T \propto T/T_0$). A set of representative experimental values and those obtained from the classical dependence on temperature are also listed in Table 5.

III.3.1. Elastic Modulus (G'). Figures 2−6 show curves of dynamic elastic modulus (G') as a function of frequency for networks synthesized with monofunctional

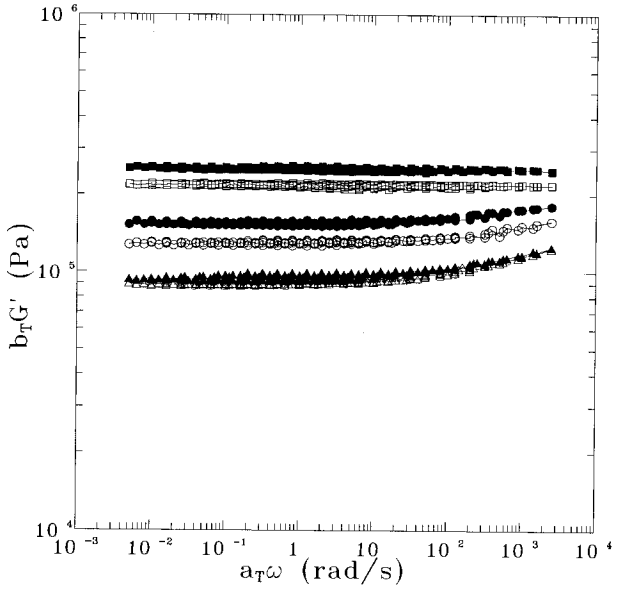

Figure 3. Master curves of elastic modulus (G') as a function of frequency (ω). $T_0 = 313$ K. Networks with monofunctional chains M2: symbols as in Figure 2.

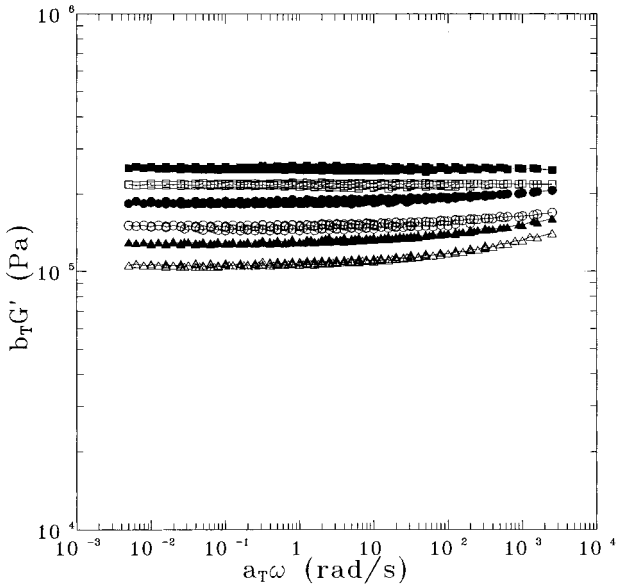

Figure 4. Master curves of elastic modulus (G') as a function of frequency (ω). $T_0 = 313$ K. Networks with monofunctional chains M3: symbols as in Figure 2.

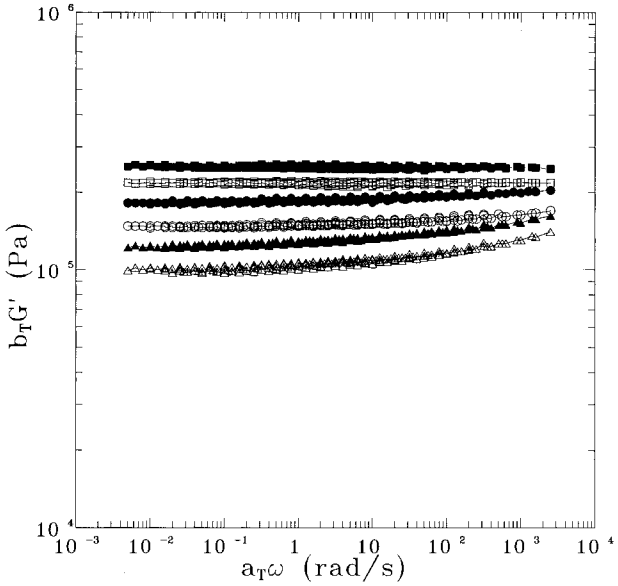

Figure 5. Master curves of elastic modulus (G') as a function of frequency (ω). $T_0 = 313$ K. Networks with monofunctional chains M4: symbols as in Figure 2.

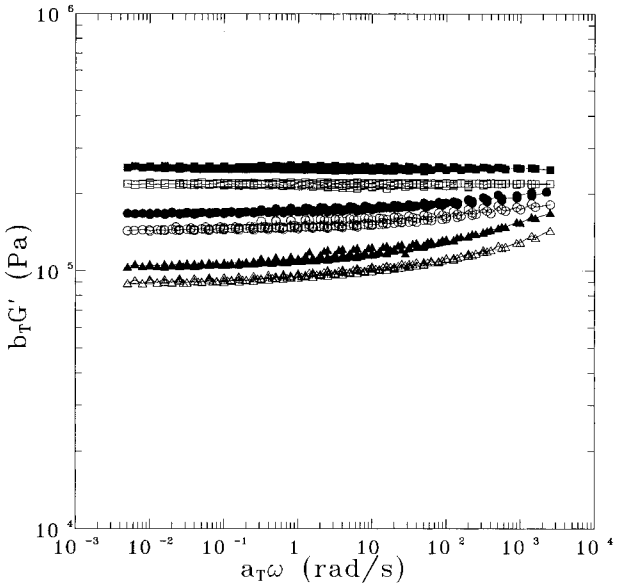

Figure 6. Master curves of elastic modulus (G') as a function of frequency (ω). $T_0 = 313$ K. Networks with monofunctional chains M5: symbols as in Figure 2.

prepolymers M1−M5 and trifunctional and tetrafunctional cross-linkers. Elastic moduli of networks prepared without pendant chains are also plotted. Results show a marked reduction in the elastic moduli of networks prepared with increasing amounts of pendant chains and a smaller decrease with cross-linking functionality. The first result is due to the reduction in the concentration of elastically active chains (ν). When the weight fraction of pendant chains in the network is increased upon the addition of increasing amounts of monofunctional chains in the reaction mixture, the concentration of elastic networks chains is reduced. This affects G' at all frequencies. A second effect is attributed to lowering of the modulus with increasing fluctuation of junction points. The elastic modulus of the networks prepared with tetrafunctional cross-linker, where fluctuation of junction points was more restricted, was always higher than that of the equivalent networks obtained with the trifunctional cross-linker. This confirms the validity of the ($\nu - \mu$) term in molecular theories and previous results obtained from tensile experiments on silicone rubbers.[4]

Experimental values of low-frequency elastic modulus and theoretical values corresponding to phantom theory (eq 1), affine deformation (eq 2), and those obtained considering the contribution of trapped entanglements (eq 4) are presented in Table 6. Values of ν, μ, and T_e were calculated using the recursive method, based on formulation data and the maximum extent of reaction obtained experimentally.[1] As shown in Table 6, elastic moduli of networks without pendant chains, measured at low frequencies, where G' is independent of ω, are in very good agreement with values calculated from the theory of elasticity when the contribution of molecular entanglements is taken into account (eq 4). Values of $h = 1$ and $G_e = G_N°$ were used in all calculations.

Table 6. Elastic Modulus Measured at Low Frequencies and Theoretically Predicted Values

		G (MPa)			
sample	cross-linker	exptl	νRT (eq 2)	$(\nu-\mu)RT$ (eq 1)	$(\nu-\mu)RT + T_eG_N°$ (eq 4, $h = 1$)
00−F3−0	A_3	0.214	0.151	0.050	0.197
00−F3−0	A_3	0.217	0.143	0.047	0.186
00−F4−0	A_4	0.252	0.194	0.088	0.245
M1−F3−20	A_3	0.120	0.072	0.024	0.116
M2−F3−20	A_3	0.129	0.082	0.027	0.126
M3−F3−20	A_3	0.147	0.079	0.026	0.129
M4−F3−20	A_3	0.147	0.083	0.028	0.134
M5−F3−20	A_3	0.144	0.084	0.028	0.133
M1−F4−20	A_4	0.158	0.107	0.043	0.147
M2−F4−20	A_4	0.154	0.101	0.041	0.131
M3−F4−20	A_4	0.185	0.115	0.048	0.156
M4−F4−20	A_4	0.182	0.124	0.052	0.175
M5−F4−20	A_4	0.157	0.119	0.050	0.161
M1−F3−33	A_3	0.076	0.044	0.015	0.081
M2−F3−33	A_3	0.089	0.058	0.019	0.102
M3−F3−33	A_3	0.106	0.053	0.018	0.093
M4−F3−33	A_3	0.101	0.054	0.018	0.099
M5−F3−33	A_3	0.091	0.055	0.018	0.099
M1−F4−33	A_4	0.135	0.091	0.037	0.130
M2−F4−33	A_4	0.094	0.082	0.033	0.120
M3−F4−33	A_4	0.128	0.084	0.034	0.127
M4−F4−33	A_4	0.123	0.097	0.040	0.142
M5−F4−33	A_4	0.106	0.076	0.031	0.103

Networks with pendant chains also show an excellent agreement between experimental and calculated elastic moduli (taking into account the contribution of trapped entanglements). An average value of *h*, the empirical parameter introduced by Graessley, for all networks prepared in this work is 0.865 ± 0.175, which is in good agreement with values previously reported for networks cured in bulk and in solution.[3] For each set of networks with approximately the same weight fraction of monofunctional chains, low-frequency elastic modulus (Table 6) has a maximum value for networks prepared with monofunctional chains M3 or M4.

Significant differences are also observed for the frequency dependence of networks with pendant chains. An increase in elastic modulus at high frequencies is observed for networks with pendant chains, while perfect networks formed exclusively with elastically active chains are almost frequency independent. This is more evident for networks with pendant chains of higher molecular weights. Values of G' increase at high frequencies because pendant chains behave as elastic chains when the entanglements involved cannot relax at those frequencies, acting then as additional cross-linking points.

III.3.2. Loss Modulus (G''). Figures 7 and 8 show values of loss modulus as a function of frequency at the reference temperature (40 °C) for networks synthesized with a weight fraction of monofunctional chains of ∼0.20. Loss modulus and relaxation times grow with an increase in the molecular weight of the pendant chains. Longer monofunctional chains, such as M4 and M5, do not relax completely in the range of frequencies analyzed. Figures 9 and 10 show values of G'' corresponding to networks prepared with a weight fraction of monofunctional chains of ∼0.33. In this case, G'' values are higher than those obtained with a weight fraction of monofunctional chains of 0.2. Also, longer chains do not relax in the range of frequencies studied. G'' values of networks without pendant chains were so low that they could not be measured in the range of frequencies and temperatures explored.

Terminal relaxation times depend on the concentration of pendant chains, their size, and the functionality of junction points. Higher concentrations of pendant

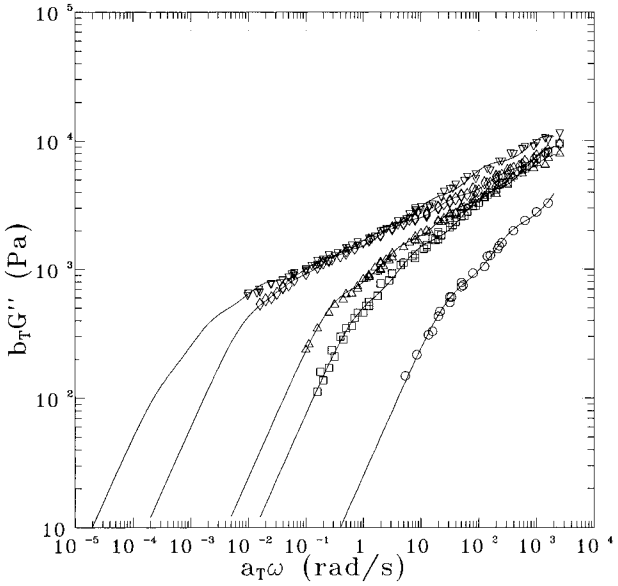

Figure 7. Master curves of loss modulus (G'') as a function of frequency (ω). $T_0 = 313$ K. Networks with ∼20 wt % of monofunctional chains and trifunctional cross-linking points: (○) monofunctional chains M1; (□) monofunctional chains M2; (△) monofunctional chains M3; (◊) monofunctional chains M4; and (▽) monofunctional chains M5. The solid lines are the predictions of eq 9 with the discrete relaxation spectrum of Table 7.

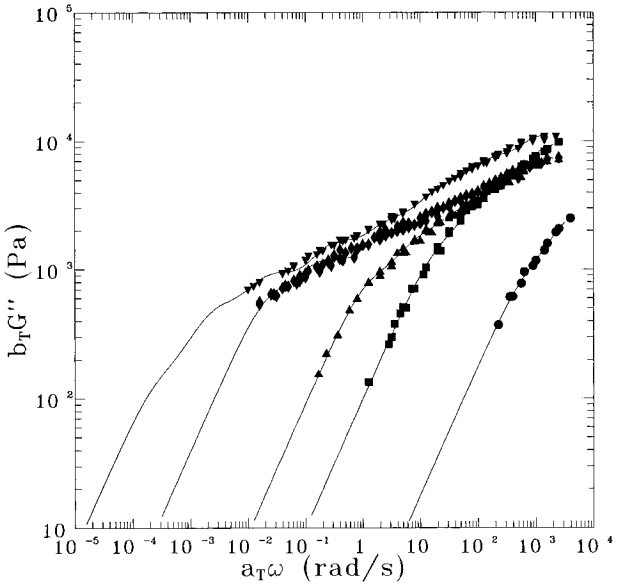

Figure 8. Master curves of loss modulus (G'') as a function of frequency (ω). $T_0 = 313$ K. Networks with ∼20 wt % of monofunctional chains and tetrafunctional cross-linking points: (●) monofunctional chains M1; (■) monofunctional chains M2; (▲) monofunctional chains M3; (♦) monofunctional chains M4; and (▼) monofunctional chains M5. The solid lines are the predictions of eq 9 with the discrete relaxation spectrum of Table 7.

chains result in larger relaxation times. The same effect is observed when the functionality of the cross-linking points is decreased.

Based on the reptation theory proposed by de Gennes,[17] pendant chains must contribute to nonequilibrium viscoelastic properties at frequencies higher than the inverse of reptation time (λ_N). Figures 7−10 show that longer pendant chains, such as M4 and M5, are relatively far from the terminal relaxation zone, where G'' is directly proportional to frequency. On the othe hand, networks containing shorter pendant chains, such as

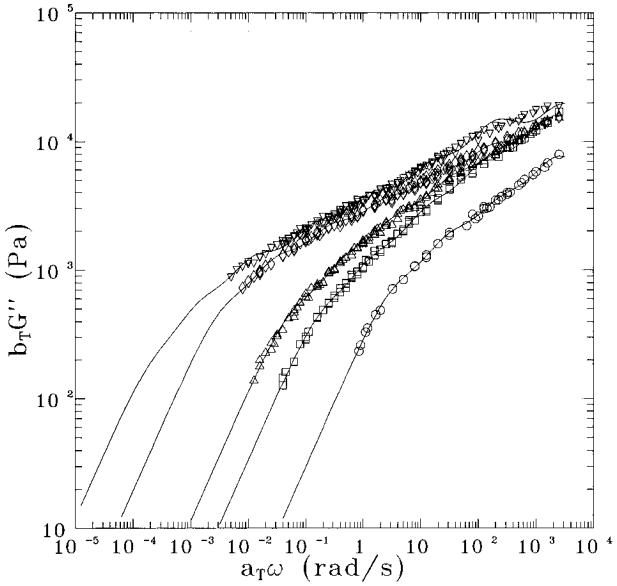

Figure 9. Master curves of loss modulus (G'') as a function of frequency (ω). T_0 = 313 K. Networks with ~33 wt % of monofunctional chains and trifunctional cross-linking points: (○) monofunctional chains M1; (□) monofunctional chains M2; (△) monofunctional chains M3; (◇) monofunctional chains M4; and (▽) monofunctional chains M5. The solid lines are the predictions of eq 9 with the discrete relaxation spectrum of Table 8.

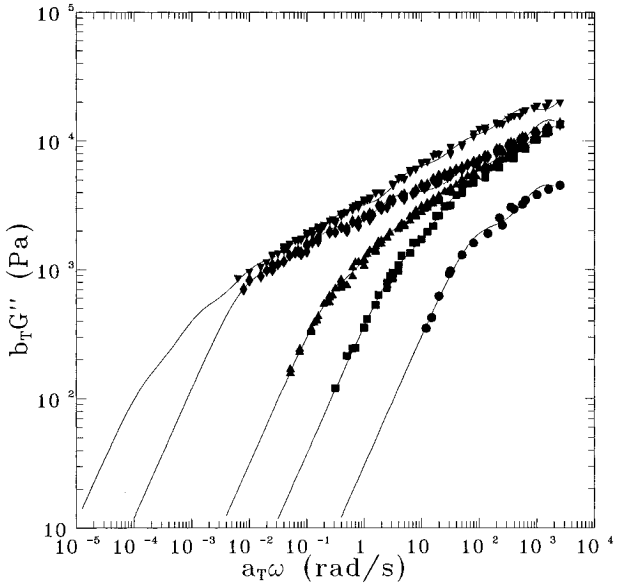

Figure 10. Master curves of loss modulus (G'') as a function of frequency (ω). T_0 = 313 K. Networks with ~33 wt % of monofunctional chains and tetrafunctional cross-linking points: (●) monofunctional chains M1; (■) monofunctional chains M2; (▲) monofunctional chains M3; (♦) monofunctional chains M4; and (▼) monofunctional chains M5. The solid lines are the predictions of eq 9 with the discrete relaxation spectrum of Table 8.

M1−M3, begin to display the terminal zone in the range of frequencies studied.

The time necessary for reptation of a pendant chain is, according to Pearson and Helfand,[28]

$$\lambda_N = \lambda_0 N^{3/2} \exp(\nu' N) \tag{8}$$

where λ_N is the reptation time, λ_0 is associated with the maximum relaxation time of a chain constituted of N_e monomers in Rouse's model, N is the number of entanglements in which a pendant chain is involved, and ν' is a constant that depends on the coordination number of the network.

Table 7. Theoretical Terminal Relaxation Time of Pendant Chains in Networks with ~20 Wt % of Monofunctional Chains and Calculated Parameters for a Generalized Maxwell Mode Expression of G''

		$f = 3$		$f = 4$	
polymer	N	λ_i (s)	η_i (Pa·s)	λ_i (s)	η_i (Pa·s)
M1	3.3	7.2×10^{-5}	1.67	1.7×10^{-4}	8.90×10^{-1}
		2.1×10^{-3}	5.62	1.4×10^{-3}	9.10×10^{-1}
		2.3×10^{-2}	1.80×10^{1}		
M2	6.5	5.1×10^{-4}	8.80	4.9×10^{-4}	8.60
		7.5×10^{-3}	3.87×10^{1}	6.1×10^{-3}	3.20×10^{1}
		9.2×10^{-2}	1.80×10^{2}	4.5×10^{-2}	5.91×10^{1}
		9.6×10^{-1}	5.35×10^{3}		
M3	7.8	3.9×10^{-4}	5.47	4.2×10^{-5}	5.40
		3.1×10^{-3}	1.68×10^{1}	3.3×10^{-4}	1.80×10^{1}
		2.5×10^{-2}	9.10×10^{1}	2.0×10^{-2}	5.90×10^{1}
		2.2×10^{-1}	4.12×10^{2}	1.0×10^{-1}	1.88×10^{2}
		2.4	1.92×10^{3}	7.0×10^{-1}	6.46×10^{2}
M4	11.5	3.9×10^{-4}	6.50	4.9×10^{-4}	6.50
		3.5×10^{-3}	2.31×10^{1}	4.7×10^{-3}	3.05×10^{1}
		2.7×10^{-2}	1.17×10^{2}	4.1×10^{-2}	1.55×10^{2}
		2.4×10^{-1}	7.45×10^{2}	3.7×10^{-1}	1.00×10^{3}
		2.4	4.06×10^{3}	4.8	8.09×10^{3}
		1.6×10^{1}	1.36×10^{4}	3.7×10^{1}	3.00×10^{4}
		8.3×10^{1}	4.15×10^{4}		
M5	15.4	5.6×10^{-4}	1.16×10^{1}	6.8×10^{-4}	1.34×10^{1}
		6.7×10^{-3}	5.84×10^{1}	6.0×10^{-3}	5.25×10^{1}
		6.4×10^{-2}	2.82×10^{2}	4.2×10^{-2}	2.29×10^{2}
		6.4×10^{-1}	1.47×10^{3}	3.6×10^{-1}	1.00×10^{3}
		5.4	7.86×10^{3}	3.3	7.24×10^{3}
		4.9×10^{1}	5.10×10^{4}	4.1×10^{1}	5.22×10^{4}
		3.5×10^{2}	1.75×10^{5}	3.5×10^{2}	2.25×10^{5}
		2.5×10^{3}	2.75×10^{5}	3.3×10^{3}	4.00×10^{5}

The loss modulus of networks containing M1−M3 monofunctional chains was fitted to a generalized Maxwell model expression (solid lines in Figures 7−10). The number of models used in each case depends on the window of frequencies covered by the measurements, and it was picked to be the minimum number necessary to obtain a smooth fit of the data. For each mode, two parameters were fitted (η_i and λ_i) in order to obtain the theoretical G'' values:

$$G''(\omega_j) = \sum_{i=1}^{N} \frac{\eta_i \omega_j}{1 + (\lambda_i \omega_j)^2} \tag{9}$$

This was done by minimizing the difference between the predicted and measured moduli at all frequencies ω_j. If we denote the measured modulus by G''_j and the predicted one by $G''(\omega_j)$, then the quantity to be minimized is

$$F_{obj} = \sum_{j=1}^{N} (\log G''_j - \log G''(\omega_j))^2 \tag{10}$$

The values of η_i and λ_i that gave the best fit are presented in Tables 7 and 8 for networks containing ~20 and ~33 wt % of monofunctional chains, respectively.

de Gennes suggested that the longest (terminal) relaxation time of a pendant chain depends exponentially on the chain length. To verify his hypothesis, we can rearrange eq 8 in the following form:

$$\ln\left(\frac{\lambda_N}{N^{3/2}}\right) = \ln \lambda_0 + \nu' N \tag{11}$$

Table 8. Theoretical Terminal Relaxation Time of Pendant Chains in Networks with ~33 Wt % of Monofunctional Chains and Calculated Parameters for a Generalized Maxwell Mode Expression of G''

		$f = 3$		$f = 4$	
polymer	N	λ_i (s)	η_i (Pa·s)	λ_i (s)	η_i (Pa·s)
M1	3.3	3.6×10^{-4}	5.15	6.2×10^{-4}	5.50
		3.7×10^{-3}	1.58×10^{1}	9.1×10^{-3}	2.50×10^{1}
		2.9×10^{-2}	6.74×10^{1}		
		2.4×10^{-1}	2.10×10^{2}		
M2	6.5	4.5×10^{-4}	1.35×10^{1}	3.5×10^{-4}	8.60
		6.5×10^{-3}	6.71×10^{1}	3.0×10^{-3}	2.30×10^{1}
		6.5×10^{-2}	2.51×10^{2}	2.1×10^{-2}	1.04×10^{2}
		5.9×10^{-1}	8.64×10^{2}	2.2×10^{-1}	2.39×10^{2}
		4.2	2.20×10^{3}		
M3	7.8	4.3×10^{-4}	1.22×10^{1}	4.8×10^{-4}	1.17×10^{1}
		3.8×10^{-3}	3.73×10^{1}	5.6×10^{-3}	4.84×10^{1}
		2.7×10^{-2}	1.79×10^{2}	4.2×10^{-2}	1.97×10^{2}
		2.3×10^{-1}	7.50×10^{2}	3.3×10^{-1}	7.68×10^{2}
		1.7	2.58×10^{3}	2.7	2.12×10^{3}
		1.4×10^{1}	7.97×10^{3}		
M4	11.5	4.9×10^{-4}	1.39×10^{1}	5.7×10^{-4}	1.57×10^{1}
		5.7×10^{-3}	7.06×10^{1}	9.4×10^{-3}	1.00×10^{2}
		4.7×10^{-2}	3.33×10^{2}	6.6×10^{-2}	1.77×10^{2}
		3.9×10^{-1}	1.78×10^{3}	2.8×10^{-1}	1.39×10^{3}
		3.4	9.83×10^{3}	3.4	1.00×10^{4}
		3.0×10^{1}	4.93×10^{4}	2.6×10^{1}	2.41×10^{4}
		2.3×10^{2}	1.35×10^{5}	9.4×10^{1}	8.50×10^{4}
M5	15.4	2.9×10^{-4}	1.07×10^{1}	3.1×10^{-5}	6.00
		4.6×10^{-3}	1.07×10^{2}	1.9×10^{-3}	4.81×10^{1}
		5.7×10^{-2}	5.45×10^{2}	1.6×10^{-2}	1.95×10^{2}
		6.5×10^{-1}	3.56×10^{3}	1.4×10^{-1}	1.11×10^{3}
		6.2	1.94×10^{4}	1.6	5.99×10^{3}
		7.1×10^{1}	1.30×10^{5}	9.5	1.93×10^{4}
		6.0×10^{2}	4.00×10^{5}	7.4×10^{1}	1.00×10^{5}
		3.9×10^{3}	6.50×10^{5}	6.3×10^{2}	3.50×10^{5}
				5.2×10^{3}	6.50×10^{5}

The values of the longest relaxation time obtained in the fitting procedure along with eq 11 are shown in Figure 11 for chains M1, M2, and M3. Values of λ_0 and ν' obtained from the equation are presented in Table 9. Both λ_0 and ν' values seem to be a function of cross-linking points functionality and cross-linking density of the networks. ν' is close to 0.6 for trifunctional networks and close to 1.0 for tetrafunctional ones. λ_0 values increase with decreasing cross-linking densities and functionality of cross-linking points.

Extrapolating eq 11 permits us to obtain values of λ_N for heavier pendant chains, such as M4 and M5. Experimental data of the loss modulus were then fitted using the generalized Maxwell model expression (eq 9), fixing the longest relaxation time to the value obtained by the extrapolation. The results are shown in Figures 7−10. As can be seen, experimental values of G'' for networks containing M4 and M5 chains are close to the relaxation zone, but this zone is not achieved in the window of frequencies covered by the present work.

Relaxation times of linear pendant chains are then in good agreement with an exponential dependence on the molecular weight or the length of the chains, in analogy with what happens for star-branched polymers.

IV. Conclusions

Model networks with controlled amounts of monodisperse pendant chains have been studied. It was found that pendant chains decrease elastic properties due fundamentally to the reduction in the amount of elastically active chains present in the resulting network. The low-frequency elastic moduli of these networks are coincident with equilibrium values predicted by the theory of elasticity if the contribution of trapped entanglements is taken into account. Values of the elastic moduli obtained from swelling experiments also show excellent agreement with theoretical values, again considering the contribution of trapped entanglements. The present work has also demonstrated that pendant chains contribute to the high-frequency elastic modulus in a proportion that depends on their molecular weight. At high frequencies, pendant chains behave as additional elastic chains because the entanglements involved cannot relax in that range of time or frequency. Networks with the same concentration of elastically active chains but prepared with a tetrafunctional cross-linker show a higher elastic modulus than those obtained with a trifunctional one because of the lower fluctuation of junction points.

However, the most important part of the present paper is the quantification of the influence of pendant chains on loss modulus (G''). It can be concluded that loss modulus depends significantly on the concentration and molecular weight of the dangling ends present in a network. Values of relaxation times obtained from G'' values are consistent with an exponential dependence of the relaxation times of pendant chains on molecular weight. These results are consistent with molecular theories proposed by de Gennes and developed by Pearson and Helfand.

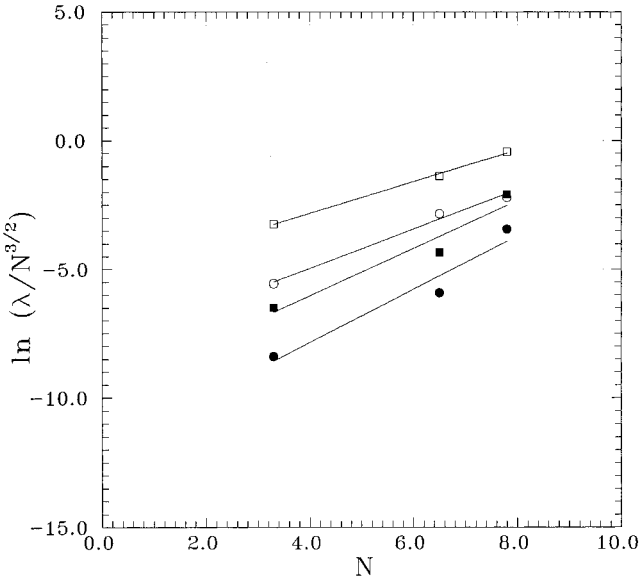

Figure 11. Longest relaxation time (λ_N) for pendant chains M1, M2, and M3 as a function of the number of entanglements. Networks with ~20 wt % of monofunctional chains: (○) trifunctional cross-linking points and (●) tetrafunctional cross-linking points. Networks with ~33 wt % of monofunctional chains: (□) trifunctional cross-linking points and (■) tetrafunctional cross-linking points.

Table 9. Maximum Relaxation Time of a Chain Composed of N_e Monomers in Rouse's Model (λ_0) and Coordination Number of the Network (ν') Obtained from Eq 11

	networks with 20 wt % of pendant chains		networks with 33 wt % of pendant chains	
	$f = 3$	$f = 4$	$f = 3$	$f = 4$
ν'	0.76	1.04	0.61	0.92
λ_0 (s)	3.3×10^{-4}	6.1×10^{-6}	5.1×10^{-3}	6.1×10^{-5}

Acknowledgment. We express our gratitude to the National Research Council of Argentina (CONICET), which supported this work.

References and Notes

(1) Vallés, E. M.; Macosko, C. W. *Macromolecules* **1979**, *12*, 673.
(2) Bibbó, M. A.; Vallés, E. M. *Macromolecules* **1984**, *17*, 360.
(3) Vallés, E. M.; Rost, E. J.; Macosko, C. W. *Rubber Chem. Technol.* **1984**, *57*, 55.
(4) Mark, J. E. *Pure Appl. Chem.* **1981**, *53*, 1495.
(5) Vallés, E. M.; Macosko, C. W. *Rubber Chem. Technol.* **1976**, *49*, 1232.
(6) Mark, J. E. *Acc. Chem. Res.* **1985**, *18*, 202.
(7) Mark, J. E.; Sullivan, J. L. *J. Chem. Phys.* **1976**, *66*, 1006.
(8) Gottlieb, M.; Macosko, C. W.; Benjamin, G. S.; Meyers, K. O.; Merrill, E. W. *Macromolecules* **1981**, *14*, 1039.
(9) Flory, P. J. *Polym. J.* **1985**, *1*, 1.
(10) Flory, P. J. *Principles of Polymer Chemistry*; Cornell University Press: Ithaca, NY, 1953.
(11) Dossin, L. M.; Graessley, W. W. *Macromolecules* **1979**, *12*, 123.
(12) Ferry, J. D. *Viscoelastic Properties of Polymers*; Wiley: New York, 1980.
(13) Graessley, W. W. *Adv. Polym. Sci.* **1974**, *16*, 1.
(14) Langley, N. R. *Macromolecules* **1968**, *1*, 348.
(15) Pearson, D. S.; Graessley, W. W. *Macromolecules* **1980**, *13*, 1001.
(16) Tsenoglou, c. *Macromolecules* **1989**, *22*, 284.
(17) de Gennes, P. G. *Scaling Concepts in Polymer Physics*; Cornell University Press: Ithaca, NY, 1979.
(18) Curro, J. G.; Pincus, P. *Macromolecules* **1983**, *16*, 559.
(19) Villar, M. A.; Bibbó, M. A.; Vallés, E. M. *J. Appl. Polym. Sci.—Appl. Polym. Symp.* **1991**, *49*, 115.
(20) Villar, M. A.; Bibbó, M. A.; Vallés, E. M. *J. Macromol. Sci.—Pure Appl. Chem.* **1992**, *A29*, 391.
(21) Villar, M. A.; Bibbó, M. A.; Vallés, E. M. *Macromolecules* **1996**, *29*, 4072 (preceding paper in this issue).
(22) Flory, P. J.; Rehner, J. *J. Chem. Phys.* **1943**, *11*, 521.
(23) Flory, P. J. *J. Chem. Phys.* **1950**, *18*, 108.
(24) Gottlieb, M.; Herskowitz, M. *Macromolecules* **1981**, *14*, 1468.
(25) Patel, S. K.; Malone, S.; Cohen, C.; Gillmor, J. R.; Colby, R. H. *Macromolecules* **1992**, *25*, 5241.
(26) Baumgaertel, M.; Soskey, P. R.; Winter, H. H. *IRIS: Innovative Rheological Interface Software*; University of Massachusetts, Amherst, MA, 1990.
(27) Williams, M. L.; Landel, R. F.; Ferry, J. D. *J. Am. Chem. Soc.* **1955**, *77*, 3701.
(28) Pearson, D. S.; Helfand, E. *Macromolecules* **1984**, *17*, 888.

MA9506602